

Photons and low-mass dileptons: results from PHENIX

Itzhak Tserruya (for the PHENIX Collaboration)¹

Weizmann Institute of Science, Rehovot, Israel

Abstract

Most recent PHENIX results on electromagnetic probes are presented including first preliminary results obtained with the Hadron Blind Detector (HBD) on e^+e^- invariant mass spectra from Au+Au collisions at $\sqrt{s_{NN}} = 200$ GeV.

1. Introduction

The potential of electromagnetic probes (real and virtual photons) to characterize the strongly interacting quark gluon plasma is well known since it was first pointed out by Shuryak [1]. They are unique in providing information about the plasma temperature, the in-medium properties of hadrons and the mechanism of chiral symmetry restoration [2]. The PHENIX detector was designed with special emphasis on the measurement of such probes [3] and has produced the first RHIC results on dileptons [4] and direct photons [5]. Capitalizing on the flexibility of the RHIC facility, PHENIX is engaged in a systematic study of electromagnetic probes. In these proceedings, I present the most recent PHENIX results on these probes, including the nuclear modification factor R_{AA} and the elliptic flow v_2 of direct photons in Au+Au collisions, the measurement of direct photons in d+Au collisions and the first results obtained with the HBD on the measurement of e^+e^- pairs in Au+Au collisions at $\sqrt{s_{NN}} = 200$ GeV.

2. Nuclear modification factor R_{AA} of direct photons

The R_{AA} of direct photons up to $p_T = 20$ GeV/c was first reported by the PHENIX experiment [6]. The preliminary results showed an intriguing suppression trend at high p_T , above ~ 12 GeV/c, albeit with very large statistical and systematic uncertainties, that triggered discussions about possible initial state and isospin effects [7]. To qualitatively improve this result, the R_{AA} was recalculated using the statistically improved 2006 p+p data [8] together with a reanalysis of the Au+Au data that combines the information of both the PbGl and PbSc calorimeters. The final results presented in Fig. 1 show that R_{AA} is consistent with 1 up to $p_T = 20$ GeV/c and for all centralities expressed by the number of participant nucleons N_{part} [9] thus resolving the long-standing issue of the behavior of the direct photons R_{AA} at high p_T .

¹A list of members of the PHENIX Collaboration and acknowledgements can be found at the end of this issue.

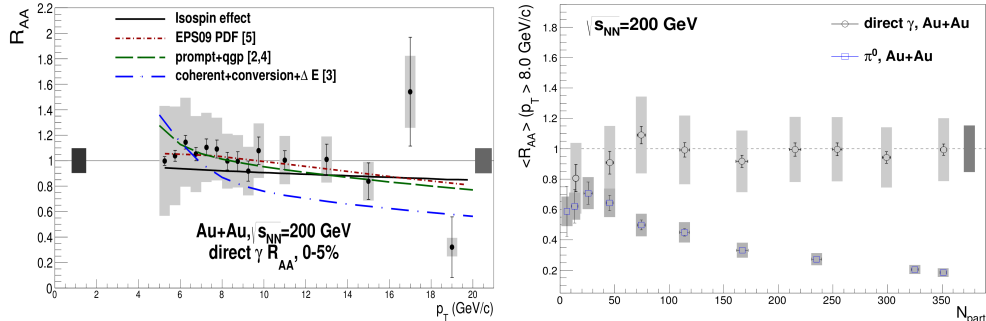


Figure 1: Left: R_{AA} vs. p_T of direct photons in central Au+Au collisions at $\sqrt{s_{NN}} = 200$ GeV. Right: R_{AA} vs. N_{part} of direct photons and π^0 for $p_T > 8$ GeV/c in Au+Au collisions at $\sqrt{s_{NN}} = 200$ GeV. For more details about the data and curves see [9].

3. Direct photons in d+Au

PHENIX has measured direct photons in p+p and Au+Au collisions at $\sqrt{s_{NN}} = 200$ GeV[5]. The p+p yield is well reproduced by NLO pQCD calculations down to $p_T = 1$ GeV/c, whereas the Au+Au data exhibit a strong excess of photons (in the p_T range of 1-3 GeV/c) beyond the p+p yield scaled by the number of binary collisions N_{coll} . This excess has an exponential shape with a slope parameter $T = 221 \pm 19^{stat} \pm 19^{syst}$ MeV in central (0-20%) collisions and has been interpreted as thermal radiation from the medium thus providing the first information about the temperature of the system averaged over the space-time evolution of the collision. Using hydrodynamical models one can infer an initial temperature of $T_{ini} = 300$ to 600 MeV depending on the assumed formation time ($\tau = 0.6$ -0.15 fm/c) of the system.

This is a seminal result. In order to further strengthen the interpretation in terms of thermal radiation, PHENIX measured the direct photons in d+Au collisions to check whether the observed excess in Au+Au collisions could originate from cold nuclear matter effects in the initial state. The direct photons in d+Au were measured via three independent methods: virtual photons, π^0 tagging and the statistical subtraction [10]. All three methods yielded consistent results as shown in the left panel of Fig. 2. The figure also demonstrates that the minimum bias (MB) d+Au data are well reproduced by the fit to the p+p data scaled by N_{coll} and that there is no excess of direct photons in the p_T range of 1-3 GeV/c. The difference with the Au+Au system is better illustrated in the right panels of Fig. 2. The right upper panel demonstrates that the nuclear modification factor in d+Au collisions is consistent with unity whereas the right lower panel shows a comparison of the R_{AA} in Au+Au and d+Au collisions. The large excess of direct photons observed in Au+Au at low p_T is not observed in d+Au and one can then conclude that it is not due to initial state effects. This result reinforces the interpretation of the Au+Au excess as thermal radiation from the sQGP.

4. Direct photons v_2

PHENIX has measured the elliptic flow v_2 of direct photons in Au+Au collisions at $\sqrt{s_{NN}} = 200$ GeV [11]. The magnitude and shape of v_2 vs. p_T are very similar to those measured for pions. A large v_2 is observed at $p_T < 4$ GeV/c where the yield is dominated by thermal photons, whereas at higher p_T , where the yield is dominated by prompt photons, v_2 is consistent with

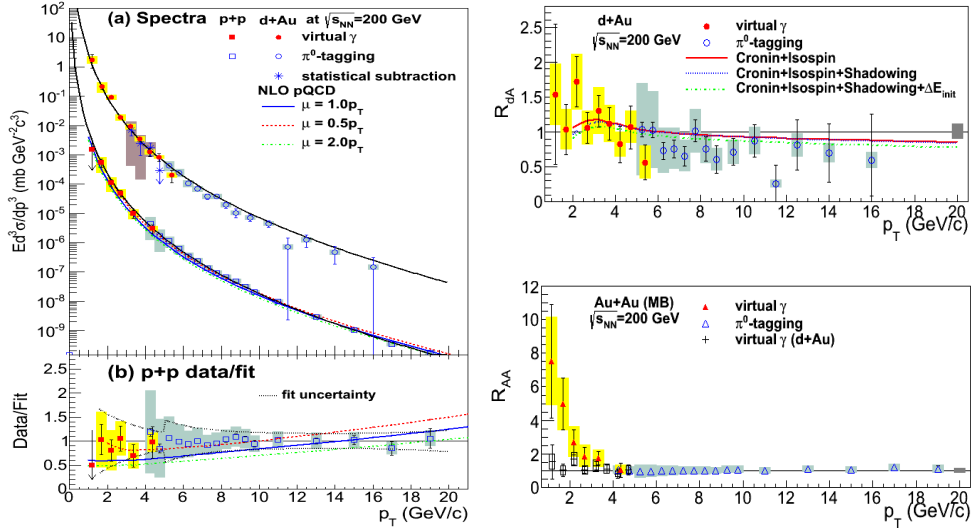


Figure 2: Left panel: Direct photon invariant spectra in p+p and minimum bias d+Au collisions at $\sqrt{s_{NN}} = 200$ GeV. The figure shows the fit of the p+p data with an empirical parametrization and the results of a NLO pQCD calculation (see [10] for details). Right upper panel: nuclear modification factor R_{AA} of direct photons in d+Au collisions. Right lower panel: Comparison of the nuclear modification factors of direct photons in minimum bias Au+Au and d+Au collisions. [10].

0 as illustrated in Fig. 3 (open circles). This is a surprising result. Thermal radiation implies early emission whereas a large v_2 implies late emission. No wonder therefore that models have difficulties in simultaneously reproducing the yield and the large v_2 values of direct photons.

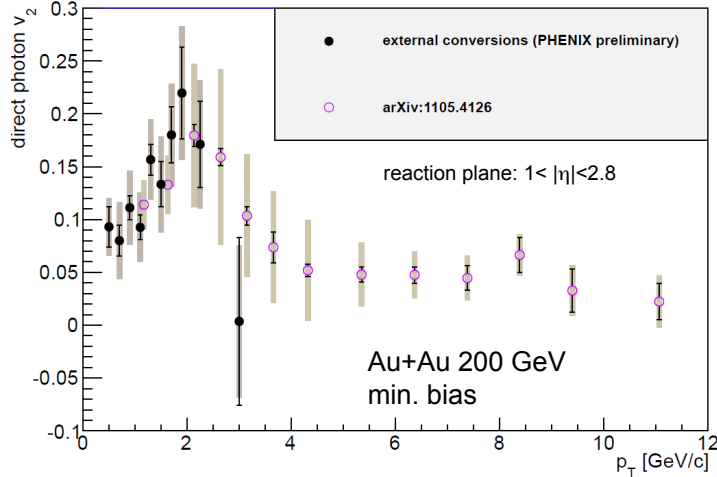


Figure 3: Direct photon v_2 published result (open circles) [11] in minimum bias Au+Au collisions at $\sqrt{s_{NN}} = 200$ GeV, compared to the new result (solid points) obtained in an independent analysis based on external conversions. The vertical error bars represent the statistical uncertainties and the shaded boxes indicate the systematic uncertainties.

The importance of this result prompted PHENIX to seek confirmation by performing a com-

pletely independent analysis with different systematic uncertainties based on external conversion photons. The new analysis allowed to extend the p_T range of the measurements down to 0.5 GeV/c and yielded consistent results with the previous one in the p_T range of overlap as illustrated in Fig. 3. This provides an important confirmation of the unexpected large v_2 values of low p_T direct photons in Au+Au collisions.

5. First dilepton results with the HBD

PHENIX has performed the first measurements of the e^+e^- pair continuum in p+p [12] and Au+Au collisions [4] at $\sqrt{s_{NN}} = 200$ GeV. The p+p results are well reproduced by the cocktail of known sources whereas the Au+Au data show a strong enhancement at low masses $m = 0.15$ - 0.75 GeV/c² with respect to a similar cocktail adjusted to Au+Au collisions. The enhancement is concentrated at the most central 0-20% collisions and reaches a factor of $7.6 \pm 0.5^{stat} \pm 1.3^{syst} \pm 1.5^{model}$ for the 0-10% centrality bin and $4.7 \pm 0.4^{stat} \pm 1.5^{syst} \pm 0.9^{model}$ for MB collisions.

In spite of numerous attempts, this result remains a challenge for theory. In particular, all models that successfully reproduced the low mass pair enhancement observed by the CERES and NA60 experiments at the SPS energies fail to reproduce the PHENIX result [2] raising the speculation of a new, yet unidentified, source of dileptons.

The PHENIX result is limited by large uncertainties, both statistical and systematic, due to the large combinatorial background and the resulting low signal to background ratio S/B and low cocktail to background ratio C/B. The latter represents an objective figure of merit for the sensitivity of the measurement to the known hadronic sources in the absence of any enhancement. For the MB data, the S/B ratio is $\sim 1/200$ and the C/B is $\sim 1/1000$. In order to qualitatively improve the measurement of low-mass dileptons, PHENIX embarked on an upgrade program. A Hadron Blind Detector (HBD) was developed with the purpose to reduce the combinatorial background.

5.1. The Hadron Blind Detector

The HBD is a windowless Cherenkov detector operated with pure CF₄, in a proximity focus configuration. The detector consists of a 50 cm long radiator directly coupled to a triple GEM detector which has a CsI photocathode evaporated on the top face of the upper-most GEM foil and pad readout at the bottom of the GEM stack. The detector is located around the beam pipe in the field free region generated by operating the inner and outer coils of the PHENIX central arms in the +- configuration. In this mode, the inner coil counteracts the main field of the outer coil creating an almost field-free region close to the vertex, extending out to ~ 50 - 60 cm in the radial direction [13, 14, 15].

The hadron blindness property of the HBD is achieved by operating the detector in the so-called reverse bias mode. In this mode, the entrance mesh is set at a lower negative voltage with respect to the top GEM and consequently the ionization electrons produced by a charged particle in the drift region between the mesh and the GEM are mostly repelled towards the mesh [14].

The choice of CF₄ as both the radiator and the detector gas in a windowless configuration results in an unprecedented large bandwidth extending from ~ 110 nm given by the CF₄ cut-off, up to ~ 210 nm given by the threshold of CsI. This large bandwidth translates into a large figure of merit N_0 and a large number of photo-electrons per electron.

The main task of the HBD is to recognize and reject tracks originating from γ conversions or π^0 Dalitz decays, where only the e^- or the e^+ is detected in the central arms. The strategy is to exploit the fact that the opening angle of electron pairs from these sources is very small

compared to the pairs from light vector mesons. In the field-free region, this angle is preserved and the pairs produce two close or overlapping hits. Therefore by applying an opening angle cut or a double amplitude cut one can reject a large fraction of the conversions and π^0 Dalitz decays, while keeping most of the signal.

The detector was successfully operated in 2009 and 2010 and collected data in p+p and Au+Au collisions, respectively. The data analysis led to a measured value of $N_0 \sim 330 \text{ cm}^{-1}$ by far higher than in any other existing gas Cherenkov counter. This translates into 20 photo-electrons per single electron incident in the detector, allowing a good separation between single and double hits, a key requirement of the HBD to identify pairs from conversions and π^0 Dalitz decays [15]. The preliminary results shown below exhibit an improvement of the S/B of ~ 5 with respect to the previous measurements without the HBD.

5.2. Analysis details

For the p+p data analysis a procedure very similar to the one described in [4, 12] was used. Significant changes were made for the Au+Au data analysis. In particular, two parallel and independent analysis streams were followed. The two streams yielded results that are in agreement within their uncertainties, thus providing a crucial consistency check. A full account of the two streams is far beyond the scope of these proceedings. Only a few aspects and details of the analysis chain that yielded the best results in terms of signal efficiency are described here.

In this first pass through the data we chose to apply strong run QA and strong fiducial cuts. This has the benefit of homogenizing the response of the central arm detectors over time thereby reducing the number of corrections necessary to account for time variations of the various subsystems. On the other hand this approach involves a large price in statistics and pair reconstruction efficiency.

CF_4 has a strong scintillation line at 160 nm, right in the middle of the HBD sensitive bandwidth. This results in a large occupancy of the detector for central collisions that requires an underlying event subtraction before attempting to identify the electrons hits in the HBD. Two different methods were used for this subtraction yielding consistent results. The HBD single electron detection efficiency achieved was $>90\%$ for the 40-60% centrality bin gradually decreasing to 65% for the most central bin of 0-10% while rejecting 90% of the fake tracks in both cases.

The HBD provides strong electron identification capability in addition to the RICH and EM-Cal detectors of the central arms. Instead of applying a series of independent one-dimensional cuts that ultimately result in a poor efficiency, we used a neural network for electron identification [16]. The neural network was trained on samples of HIJING events covering all centralities. A significant improvement of the global single electron track efficiency (of $\sim 50\%$ for the peripheral 60-92% events and $\sim 20\%$ for the most central 0-10% events) was obtained with the neural network as compared to the standard electron identification cuts. A neural network was also used to inspect the vicinity of electron hits and decide whether the HBD signal corresponds to a single or a double electron hit.

The combinatorial background was subtracted in two separate steps. First the background resulting from the random combination of e^- and e^+ in the same event was subtracted using a mixed event technique. The normalization of the unlike mixed event background is obtained by normalizing the like-sign mixed event spectrum to the like-sign foreground spectrum in a phase space region which is free from correlations (mass $> 0.55 \text{ GeV}/c^2$ to avoid cross pairs [4] and opening angle $< 120^\circ$ to avoid jet correlations). After this first step, the foreground unlike-sign

spectrum contains both correlated background pairs and signal pairs and the foreground like-sign spectra contain only correlated background pairs. In the second step, the residual like-sign spectra, corrected for the acceptance difference between $++$, $--$ and $+-$ pairs, are subtracted from the residual unlike-sign spectrum to obtain the raw signal yield [4]. This approach is relatively simple but results in a factor of $\sqrt{2}$ larger statistical error as opposed to the case in which the various background sources are determined a priori and subtracted one after the other, without relying on the measured like-sign spectra.

The raw signal is then corrected for acceptance and reconstruction efficiency to yield the invariant dilepton mass spectrum within the ideal acceptance of the PHENIX detector. Conservative systematic errors were assigned to the various steps of the analysis and in particular to the combinatorial background subtraction.

The Au+Au data were analyzed in the same five centrality bins as in the previously published PHENIX dilepton results [4]. In these proceedings we are presenting the results for peripheral (60-92%), semi-peripheral (40-60%) and semi-central (20-40%) events. Results from the two most central bins (0-10% and 10-20%) are not yet available.

5.3. Cocktail of hadronic sources

The results are compared to a cocktail containing all the known hadronic sources. The EXODUS event generator [4] is used to simulate the photonic sources (Dalitz decays of light neutral mesons: $\pi^0, \eta, \eta' \rightarrow e^+e^-\gamma$ and $\omega \rightarrow e^+e^-\pi^0$) and the non-photonic sources (di-electron decays of the light vector mesons: $\rho, \omega, \phi \rightarrow e^+e^-$). The correlated pairs from semi-leptonic decays of heavy flavor (charm and bottom) mesons are generated using the MC@NLO package [17] which calculates the initial hard scattering at the next to leading order. After generating the various sources, the cocktail is filtered through the ideal acceptance of the PHENIX detector and smeared with the detector resolution.

π^0 is the dominant electron source and also the fundamental input for EXODUS. For each centrality bin, we use π^0 p_T spectra based on PHENIX measurements of neutral and charged pions. For other mesons, the shape of the p_T distribution is obtained assuming m_T scaling. The absolute normalization is provided by the meson to π^0 ratio at high p_T [4].

The J/ψ line shape for the p+p cocktail is obtained from a full Monte Carlo simulation where J/ψ decays into e^+e^- are propagated through the full chain of reconstruction and analysis cuts using a GEANT based simulation of the PHENIX detector. For the J/ψ in Au+Au, the shape and yield are taken from the p+p measurement, the latter being scaled by N_{coll} and the measured nuclear modification factor R_{AA} [18]. Therefore the comparison cocktail vs data for the J/ψ in Au+Au is reduced to a consistency check between the previously published and the present J/ψ yields, without and with HBD, respectively.

5.4. Results

Figure 4 shows the invariant mass spectrum of e^+e^- pairs within the PHENIX detector acceptance measured in the 2009 p+p run with the HBD. The results are compared to the expected yield from the cocktail of known sources. The bottom panel shows the ratio of data to cocktail and demonstrates a good understanding of the measured spectrum. The present result is fully consistent with the previously published one without the HBD [12] and provides a crucial proof of principle for usage of the HBD. This analysis is now being repeated using all the tools of the new analysis chain developed for the Au+Au data analysis in order to fully assess the benefit of these tools.

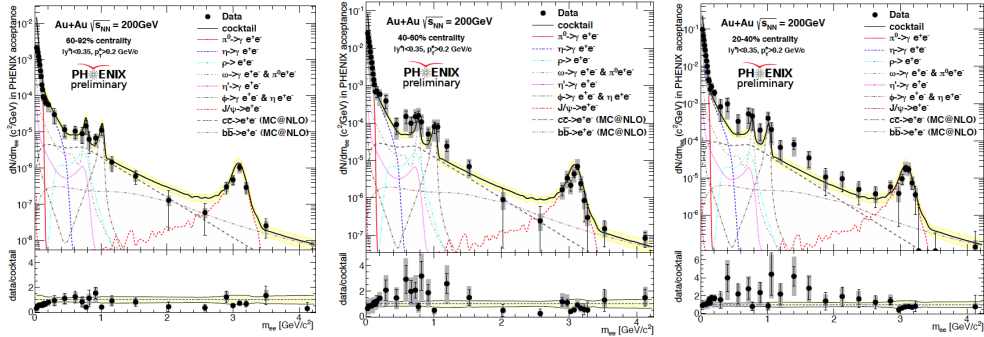


Figure 5: Invariant mass spectrum of e^+e^- pairs in Au+Au collisions at $\sqrt{s_{NN}} = 200$ GeV measured in the 2010 run with the HBD in three centrality bins. The data points show statistical (vertical bars) and systematic (shades) uncertainties separately. The shaded band represents the systematic uncertainty of the cocktail.

Figure 5 shows the invariant mass spectra of e^+e^- pairs within the PHENIX detector acceptance measured in Au+Au collisions in the 2010 run with the HBD, in three centrality bins: 60-92% (left panel), 40-60% (middle panel) and 20-40% (right panel). The results are compared to the expected yield from the cocktail of known sources, briefly described in the previous section. The bottom panels show the ratio of data to cocktail. In the most peripheral bin the measured spectrum is in quite good agreement with the expected yield. For semi-peripheral and semi-central events there seems to be a small enhancement of the measured yield with respect to the cocktail that increases with centrality, both in the low-mass region (LMR, $m = 0.15 - 0.75$ GeV/ c^2) and the intermediate mass region (IMR, $m = 1.2 - 2.8$ GeV/ c^2). However, no clear statement can be made at this stage with the present level of very conservative errors.

There are significant differences between the 2010 run with the HBD and the 2004 run without it, that prevent a direct comparison of the results. In the 2010 run the central coils were operated in the +- configuration, as opposed to ++ in 2004, resulting in larger acceptance of low p_T tracks. There is more radiative tail in the J/ψ , ϕ and ω line shapes due to the HBD material in front of the central arms. There is also a difference in the cocktails. In the 2010 run, the open heavy flavor contribution is calculated using the MC@NLO package whereas in the 2004 data analysis we used PYTHIA. This results in a calculated yield in the IMR which is $\sim 16\%$ larger

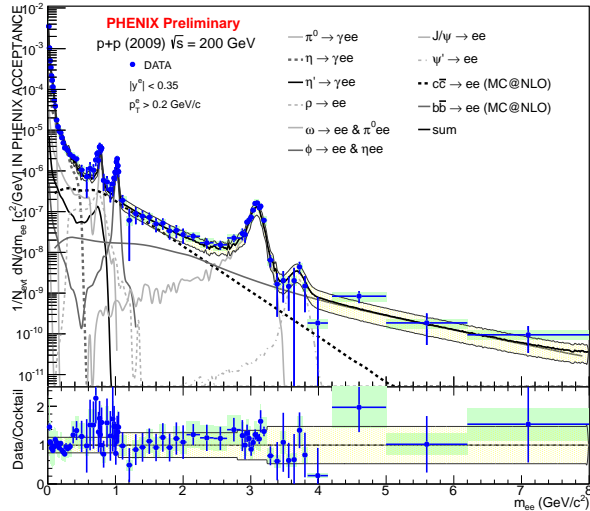


Figure 4: Invariant mass spectrum of e^+e^- pairs in p+p collisions at $\sqrt{s} = 200$ GeV measured in the 2009 run with the HBD. The data points show statistical (vertical bars) and systematic (shades) uncertainties separately. The data are compared to the expected yield from a cocktail of the known hadronic sources. The shaded band represents the systematic uncertainties of the cocktail. The bottom panel shows the data to cocktail ratio.

with the MC@NLO than with PYTHIA. To account for these differences, we compare in Fig. 6 the data/cocktail ratio for the integrated yield in the LMR and the IMR as obtained in the 2004 and 2010 runs for the three centrality bins presented here. The 2004 PYTHIA yield in the IMR is scaled up by 1.16 to account for the difference with the MC@NLO calculations. The figure shows consistent results between the two runs within their uncertainties.

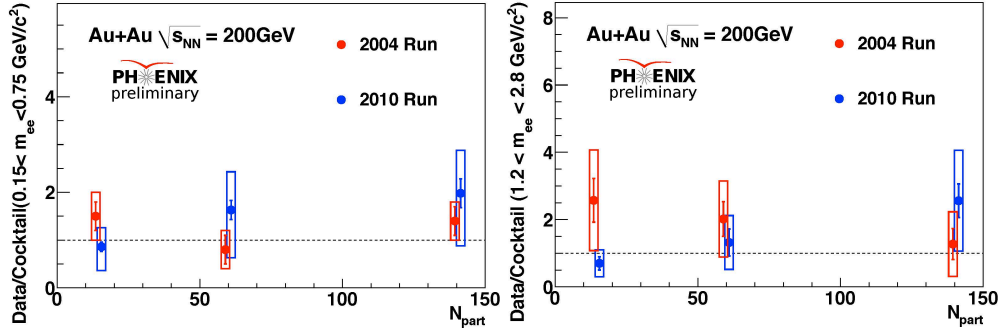


Figure 6: Comparison of the data/cocktail ratio with (2010 run) and without (2004 run) the HBD of the integrated yield in the LMR (left) and the IMR (right) as function of N_{part} .

6. Summary and outlook

PHENIX is pursuing its systematic study of electromagnetic probes exploiting the flexibility of the RHIC facility. Recent achievements presented here, include final results on R_{AA} of direct photons [9], independent confirmation of the large v_2 values of direct photons and first measurement of direct photons in d+Au collisions. The preliminary dilepton analysis using the HBD, with strong QA cuts and conservative error estimates, yielded consistent results with those previously published [4, 12]. The final analysis is expected to show a significant improvement in the statistical and systematic uncertainties and to include the two most central bins.

References

References

- [1] E.V. Shuryak, Phys. Lett. **B78**, 150 (1978).
- [2] For recent theoretical and experimental reviews see the papers of C. Gale (p. 6-74), R. Rapp et al. (p. 4-1) and I. Tserruya (p. 4-43) in "Relativistic Heavy Ion Physics", published in Landolt-Boernstein, Vol. I-23 (2010).
- [3] K. Adcox et al. (PHENIX Collaboration), Nucl. Instr. and Meth. **499**, 469 (2001).
- [4] A. Adare et al. (PHENIX Collaboration), Phys. Rev. **C81**, 034911 (2010).
- [5] A. Adare et al. (PHENIX Collaboration), Phys. Rev. Lett. **104**, 132301 (2010).
- [6] T. Awes for the PHENIX Collaboration, J. Phys. **G35**, 104007 (2008).
- [7] F. Arleo, JHEP **0609**, 015 (2006).
- [8] A. Adare et al. (PHENIX Collaboration), Phys. Rev. **D86**, 072008 (2012).
- [9] S. Afanasiev et al. (PHENIX Collaboration), Phys. Rev. Lett. **109**, 152302 (2012).
- [10] A. Adare et al. (PHENIX Collaboration), arXiv:1208.1234.
- [11] A. Adare et al. (PHENIX Collaboration), Phys. Rev. Lett. **109**, 122302 (2012).
- [12] A. Adare et al. (PHENIX Collaboration), Phys. Lett. **B670**, 313 (2009).
- [13] A. Kozlov et al, Nucl. Instr. and Meth. **A523**, 345 (2004).
- [14] Z. Fraenkel et al., Nucl. Instr. and Meth. **A546**, 466 (2005).
- [15] W. Anderson et al., Nucl. Instr. and Meth. **A646**, 35 (2011).

- [16] The neural network was implemented using the class `TMultiLayerPerceptron` from the root package:
<http://root.cern.ch/root/html530/TMultiLayerPerceptron.html>
- [17] S. Frixione and B.R. Webber, JHEP 0206:029, 2002
- [18] A. Adare et al. (PHENIX Collaboration), Phys. Rev. Lett. **98**, 232301 (2007).